Journal of Machine Engineering, 2026, Vol. 26
ISSN 1895-7595 (Print) ISSN 2391-8071 (Online)

Received*: 10 November 2025* / Accepted: *17 December 2025* / Published online: *16 January 2026*

metrology FDM,
geometric defects,
circularity multi-slice analysis

Anass EL-QEMARY[1*], Ikram KABBOURI[1],
Hamid HENNANE[1], Mouhssine CHAHBOUNI[1],
Said BOUTAHARI[1]

METROLOGICAL MODELING OF CIRCULARITY IN ADDITIVE MANUFACTURING: A HYBRID MULTI-SECTION APPROACH

This article introduces a hybrid method for assessing the circularity of cylindrical parts produced via Fused Deposition Modeling (FDM). The proposed approach combines a multi-section analysis with the generation of an adaptive reference cylinder, enabling a detailed evaluation of geometric deviations along the build axis. By segmenting the part into transverse profiles, the method captures gradual shape variations induced by the layer-by-layer nature of the additive process. This strategy enhances the understanding of form deviations linked to process parameters and stacking effects, and contributes to more reliable geometric modeling in additive manufacturing.

1. INTRODUCTION

Additive manufacturing (AM), and in particular fused deposition modeling (FDM), is attracting growing interest for the production of technical parts due to its ability to create complex geometries with a high degree of customization. Nevertheless, despite this design freedom, additive processes introduce non-negligible dimensional and geometric variability, especially on cylindrical features such as circularity and cylindricity. Additive manufacturing has transformed the manufacturing landscape by enabling the production of complex geometries that were once unachievable with conventional techniques [1].

According to [2], the circularity and cylindricity deviations observed in 3D-printed parts are strongly influenced by process parameters, in particular the build orientation and layer thickness. These geometric defects largely stem from the successive stacking of layers, thermal shrinkage, and path inaccuracies of the extrusion nozzle. As a result, a part intended to be perfectly cylindrical may exhibit, after fabrication, gradual diameter variations or

[1] Laboratory of Technology and Industrial Services, Higher School of Technology, Sidi Mohammed Ben Abdellah University, Morocco
[*] E-mail: anass.elqemary@usmba.ac.ma
https://doi.org/10.36897/jme/215771

distorted profiles of the barrel-shaped or conical type.

Traditional cylindricity inspection methods, which mainly rely on a global fit to an ideal cylinder, show their limits when it comes to detecting and analysing localized deformations or gradual variations along the height of parts. To overcome these limitations, recent studies have explored innovative approaches—most notably geometric segmentation and process-parameter optimization to improve the geometric quality of printed parts selectively [3].

In this study, we propose an innovative, hybrid inspection method that combines a multi-slice analysis using horizontal sections at different heights of the part with the progressive fitting of an adaptive cylinder reconstructed from measurement data. This work aims to capture gradual deformations better and to deliver a realistic representation of the actual cylindricity of additively manufactured parts. Conventional cylindricity inspection, which relies on a single global fit to an ideal cylinder, often proves insufficient because it smooths out the progressive and localized distortions generated during the process, thereby masking the true geometric behaviour of the printed component [2].To address these methodological limitations, we introduce a novel hybrid approach grounded in vertical segmentation of the part by successive horizontal slices, coupled with the modeling of an adaptive cylinder reconstructed from the locally fitted circles. This strategy analyses local variations in circularity along the *Z*-axis, enabling a finer and more realistic mapping of evolving deformations than conventional global fits. Recent studies, such as [4] have shown that layer-by-layer geometric analysis improves the identification of irregularities arising from the successive stacking of layers in additive manufacturing. In this vein, the proposed hybrid method virtually partitions the part into multiple horizontal sections; for each section, a circle is fitted to locally model the actual geometry, and the collection of these circles is then used to generate an adaptive cylinder that more faithfully reflects progressive deformations than a traditional global adjustment.

2. LITERATURE REVIEW

Since the early 2010, additive manufacturing (AM) has experienced rapid growth due to its ability to produce complex parts while offering significant design freedom. A study [5] provided an overview of the processes and highlighted challenges related to the geometric quality of printed parts, particularly with the fused deposition modeling (FDM) process. Similarly, the study conducted by [6] examined how layer thickness directly affects the geometric accuracy of manufactured components. In turn, [7] investigated dimensional deviations in FDM-produced parts, revealing that features such as flatness, circularity, and cylindricity are closely dependent on process parameters. A multiparametric approach was developed by [2] to measure form deviations on cylindrical parts, highlighting the critical importance of printing orientation. A slice adaptation strategy based on form tolerances was proposed by [2], aiming to improve accuracy while avoiding an increase in printing time.

The thesis titled “Contribution to the Design of Mechanisms: Tolerance Analysis with the Influence of Form Defects” [8], examines geometric tolerances by integrating form

defects through worst-case and statistical approaches, illustrated via assembly examples and non-conformity rate calculations.

An error compensation model for cylindrical shapes was developed by [9], while the study by [10] demonstrated the influence of extrusion speed on cylindricity defects. The research conducted by [11] shows that FDM process parameters, layer height, extrusion temperature, and deposition speed significantly affect the circularity and cylindricity of printed parts. A multi-criteria optimization strategy is recommended to minimize these deviations. Furthermore, the study by [12] identifies three main sources of error impacting the geometry of parts produced using Fused Deposition Modeling (FDM). The first involves inaccuracies in the movement of the extrusion system, which may distort the deposition path. The second relates to thermal deformations caused by material shrinkage during heating and cooling phases. The third source of error stems from the conversion of the CAD model into an STL file, a process based on geometric approximation through triangular facets, which can lead to dimensional fidelity loss.

Additive manufacturing enables the assembly of materials from 3D models without the need for tooling, typically layer by layer, unlike subtractive methods. However, it does not benefit from the century-long research legacy of component production that supports precision subtractive techniques. As a result, certain aspects of the manufacturing value chain, such as metrology and inspection, remain better understood in subtractive contexts and still require significant advancement in additive manufacturing [13]. The nominal shape of a layer is obtained by slicing the STL file at the desired height and connecting the points to form a theoretical contour, while the actual printed shape is reconstructed from measured points to form the real contour [14].

The Material Extrusion family of AM techniques, specifically the FDM process, was chosen for this research as it is presently one of the most used AM technologies for polymers due to the simplicity of its implementation and low cost, together with the widespread availability of desktop-type machines and compatibility with standard materials like PLA. This makes FDM a reference process due to its wide industrial and academic adoption for the metrological analysis of printed polymer parts. However, it is known to show some limitations in dimensional and form accuracy, particularly evident in functional geometries like cylinders [15]. Recent studies have highlighted that FDM-manufactured parts exhibit limited achievable accuracy, and that the digital workflow (CAD to STL conversion followed by slicing) introduces discretization errors that directly affect the final geometry [15, 16]. The selection of the FDM process in this case serves a dual purpose: to study a method that is broadly representative of current practices in polymer 3D printing, and to examine a context in which geometric deviations are sufficiently critical to require an advanced inspection method.

Recent work by [12] also demonstrated and modeled the influence of so-called 'source-process' defects on geometric quality, proving that geometric deviations observed on printed cylinders are mainly due to format STL meshing errors, thermal-mechanical shrinkage and deformation effects, and cinematic inaccuracies of the machine during layer-by-layer deposition. The aforementioned sources contribute jointly to a measurable global deviation; therefore, geometric correction of the nominal model will be required. Study [16] formalizes this observation through a modeling approach that combines systematic modes, such as radius

variation, ellipticity, and meshing effects, with a random component, thereby establishing a clear connection between process mechanisms and metrological signatures observed on cylindrical surfaces. These findings are consistent with the adopted experimental approach: by measuring the part and analysing the circularity and cylindricity cross-section by cross-section according to ISO 1101, it becomes possible to identify characteristic signatures (R(z) variability, lobbing, axis drift) that reflect deposition and shrinkage defects inherent to the FDM process.

Finally, recent literature indicates that FDM process parameters, such as extrusion temperature, printing speed, layer thickness, build orientation, and infill density, strongly affect circularity and cylindricity errors in cylindrical parts. These effects are mainly driven by thermally induced shrinkage, over- or under-extrusion phenomena, and kinematic instabilities [17]. In this context, building on the methodological foundations of studies [12] and [16], together with a detailed metrological assessment of the investigated PLA cylinder, enables a quantitative linkage between FDM-induced process defects and the measured geometric deviations. This, in turn, supports a robust and actionable diagnosis aimed at improving the conformity of printed components.

3. STUDY PURPOSE

3.1. ADAPTIVE LOCALIZED METROLOGY FOR CIRCULARITY OF PRINTED CYLINDERS

The purpose of this research is to propose an innovative and rigorous method for evaluating the circularity of cylindrical parts produced by Fused Deposition Modelling (FDM), in light of the limitations of traditional form inspection approaches. Conventional methods, which rely on global fitting of a reference cylinder, often fail to detect local shape deviations caused by the specific characteristics of the FDM process (layer stacking, thermal variations, shrinkage, etc.) Fig.1. To address these limitations, this study introduces a hybrid geometric inspection approach in 2D, structured around two complementary components: first, a multi-section analysis that extracts and examines circular profiles at various heights of the part to locally characterize form deviations; second, an adaptive modelling of the reference cylinder, constructed from the centers of the fitted sections, which accounts for axial drift and asymmetric deformations. At this stage, the proposed method enables the identification of deviations in two dimensions only, while paving the way for future extension toward full 3D modelling.

This study aims to develop a hybrid approach to geometric inspection based on two complementary components:

- A multi-section analysis that enables the extraction and examination of circular profiles distributed along various heights of the part, to locally characterize form deviations.

This will subsequently allow for the implementation of:

- An adaptive modeling of the reference cylinder, constructed from the centers of the fitted sections, to account for axial drift and asymmetric deformations.

The main aim of this study is to evaluate the circularity of additively manufactured cylindrical parts in accordance with ISO 1101. The proposed method estimates circularity by computing the maximum deviations between measured points and an adaptively generated reference cylinder. The method is demonstrated on a printed case study part, showing its potential to support a more representative inspection protocol that better captures the geometric behaviour typically observed in additively manufactured components. By addressing key challenges in circularity assessment, the approach provides a metrological framework that can be adapted to industrial precision requirements.

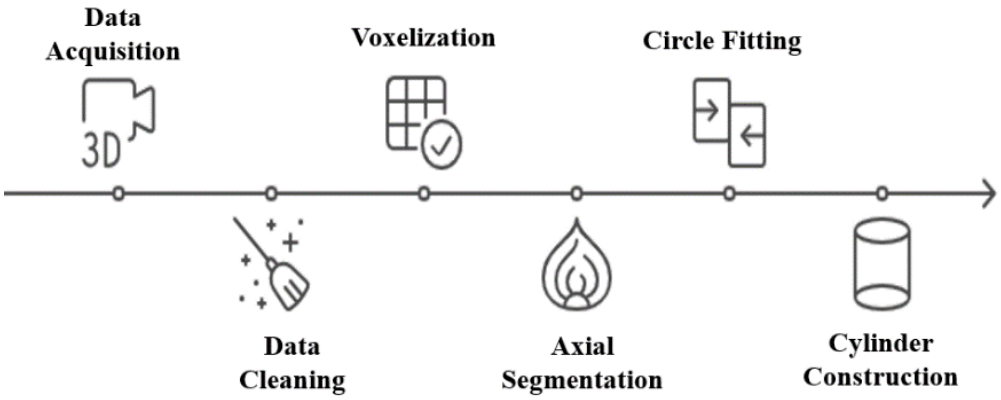

Fig. 1. Methodological diagram: multi-section analysis and adaptive cylinder

4. METHODOLOGY

4.1. EXPERIMENTAL FRAMEWORK AND POINT-CLOUD PRE-PROCESSING

The proposed methodology relies on a combination of experimental measurements and advanced geometric processing applied to a cylindrical part produced by Fused Deposition Modeling (FDM). The test specimen is a solid cylinder measuring 40 mm in diameter and 30 mm in height (Fig. 2 Left), printed in PLA using an Ultimaker-type FDM printer (Fig. 2 Right), with the following parameters:

- Nozzle: Diameter of 0.4 mm;
- Wall thickness: set at 0.4 mm;
- Deposition Speed: Adjusted to 100 mm/s;
- Infill pattern: Zigzag;
- Orientation: Vertical (Z-axis);
- Fill Rate: 100%.

This configuration allows for the reproduction of typical production conditions while highlighting potential defects associated with the FDM process.

The test part was digitized at the Innovation Center of Sidi Mohamed Ben Abdellah University using a HANDY Scan 307 structured-light 3D optical scanner (Fig. 3), generating a raw point cloud (STL format) representing its surface (Fig. 4). However, this raw cloud is

often affected by artefacts (isolated points, noise, redundancies) resulting from reflections, shadows, or instrumental limitations. To ensure data quality before geometric analysis, a rigorous pre-processing was carried out in MATLAB. This pre-processing consists of four main steps: extraction of unique points, statistical filtering of outliers, density reduction through voxelization, and axial segmentation.

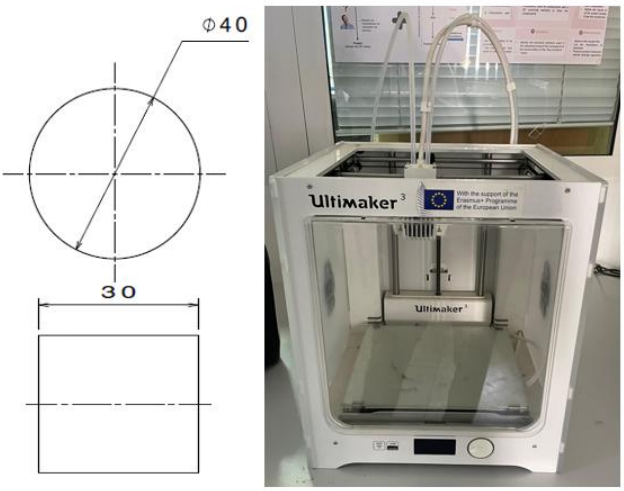

Fig. 2. (Left) The modeled part with nominal dimensions; (Right) The ULTIMAKER machine used

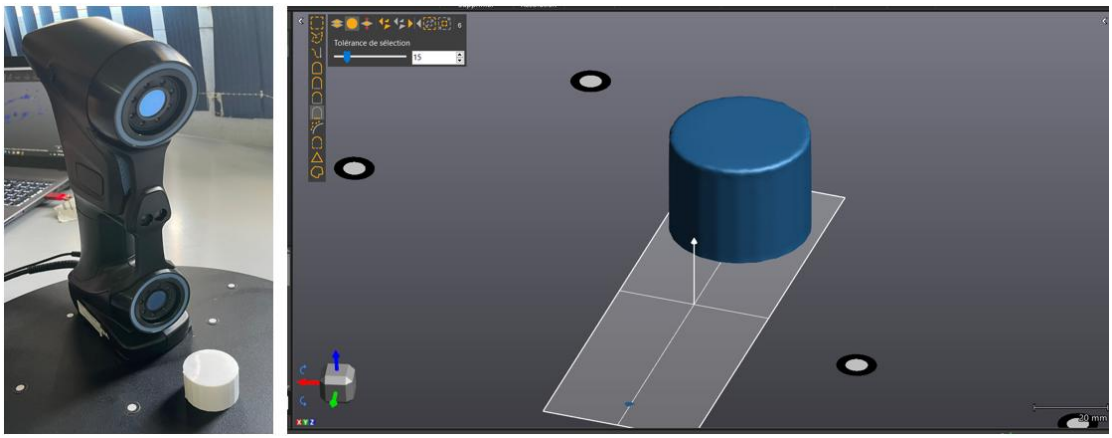

Fig. 3. (Left) HANDY Scan scanner used; (Right) scanned geometry of the studied part

First, redundant vertices from the STL triangular mesh are removed using the unique function, resulting in a refined set of coordinates. Next, a filtering process based on the average distance to the k-nearest neighbors (k = 12) is applied. Points whose average distance exceeds two standard deviations from the global mean are considered outliers and discarded, in accordance with the methods proposed in [18]. his threshold ensures a balance between robustness and the preservation of geometric details. Subsequently, the data is spatially homogenized using a voxel grid (0.1 mm), which maintains a uniform distribution while reducing the number of points to process. A similar method was discussed in [19], where the effects of density reduction on reconstruction accuracy were analysed in the context of 3D

scanning of technical parts. Furthermore, points located outside the target range were removed to retain only the lateral surface required for subsequent cylindricity analysis.

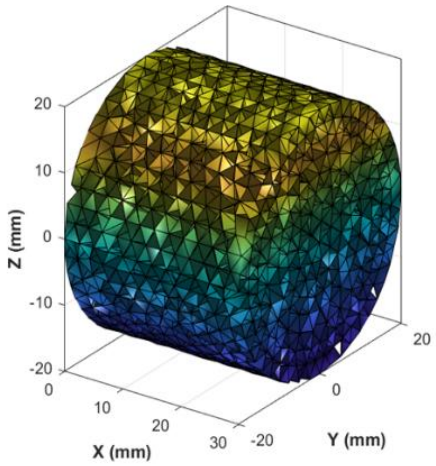

Fig. 4. Isometric view of the point cloud from digitization

The raw point cloud P, is first deduplicated using a uniqueness criterion (micrometric tolerance) to eliminate repeated vertices from the STL mesh. Outliers are then removed using a k-NN distance metric (k = 12), retaining only observations whose average distance to neighbors falls below a statistical threshold, in line with inlier/outlier identification strategies designed to make point cloud matching and processing robust to noisy data [20]. Sampling density is homogenized through isotropic voxelization (grid size Δ = 0.10 mm), a subsampling principle recently optimized to reduce redundancy while preserving local geometry [21]. The cloud is then re-centered and reoriented using Principal Component Analysis (PCA), aligning the principal axis with the Z-axis, an approach consistent with recent methods for cylinder detection and parameterization in unstructured point clouds [22]. Finally, axial segmentation (margins m_z = 0.50 mm, step Δz = 0.50 mm) produces XY sections ready for circle fitting. This step paves the way for constructing an adaptive cylinder, enabling cylindricity evaluation based on minimum zone approaches aligned with the state of the art [23–24] (Fig. 5).

4.2. POINT CLOUD PRE-PROCESSING: FROM RAW STL DATA TO CLEANED AND ALIGNED POINT CLOUDS

ALGORITHM PointCloudPreprocessing
INPUTS
  filePath : path to the STL file (e.g., “Study Part_40-30.stl”)
PARAMETERS (defaults for Ø40 × 30 mm)
  k ← 12
  Δvoxel ← 0.10 mm
  Δz ← 0.50 mm
  m_z ← 0.50 mm
  outlier ← “std”
OUTPUTS
  P_clean : cleaned, homogenized, Z-aligned point cloud (N×3)
  slices : list of slice structures; for each slice s:

s.z : axial level (mm)
s.pts : XY-projected points ($n\_s \times 2$)
s.n : number of points in the slice (n_s)
meta : metadata (center, rotation, bounds, point count, etc.)

PROCEDURE

1) Load STL
$M \leftarrow$ readSTL(filePath)
$P \leftarrow$ verticesOrSamplesOf(M)
$P \leftarrow$ UNIQUE(P)

2) Outlier filtering (k-NN)
for each point $p\_i \in P$:
$N\_i \leftarrow$ kNearestNeighbors(p_i, k)
$d\_i \leftarrow (1/k) \cdot \Sigma\_\{j \in N\_i\} \|p\_i - p\_j\|_2$
if outlier = "std":
$\mu\_d \leftarrow$ mean($\{d\_i\}$), $\sigma\_d \leftarrow$ std($\{d\_i\}$)
$I \leftarrow \{ i \mid d\_i \le \mu\_d + 2\sigma\_d \}$
else if outlier = "mad":
$m\_d \leftarrow$ median($\{d\_i\}$)
MAD $\leftarrow$ median($\{ |d\_i - m\_d| \}$)
$T \leftarrow m\_d + 3 \cdot 1.4826 \cdot$ MAD
$I \leftarrow \{ i \mid d\_i \le T \}$
$P \leftarrow P[I]$

3) Isotropic voxelization (grid of step Δvoxel)
for each p = $(x,y,z) \in P$:
$v \leftarrow (\lfloor x/\Delta\text{voxel} \rfloor, \lfloor y/\Delta\text{voxel} \rfloor, \lfloor z/\Delta\text{voxel} \rfloor)$
push p into bucket $V[v]$
$P\Delta \leftarrow \emptyset$
for each voxel V:
$\hat{c} \leftarrow$ mean($\{ p \in V \}$)
$P\Delta \leftarrow P\Delta \cup \{\hat{c}\}$
$P \leftarrow P\Delta$

4) Recenter & align (PCA)
$c \leftarrow$ mean(P)
$X \leftarrow P - c$
$\Sigma \leftarrow (1/|X|) \cdot X^T X$
$\{\lambda_1 \ge \lambda_2 \ge \lambda_3, e_1, e_2, e_3\} \leftarrow$ eig(Σ)
$R \leftarrow$ RodriguesRotation($e_1 \rightarrow \hat{z}$)
$P \leftarrow (R \cdot X^T)^T$

5) Trim Z-ends (margin)
z_min $\leftarrow$ min(P[:,3]); z_max $\leftarrow$ max(P[:,3])
$G \leftarrow \{$ indices with $z \in [$ z_min + mz , z_max − mz] $\}$
P_clean $\leftarrow P[G]$

6) Axial slicing (step Δz)
$K \leftarrow$ ceil((z_max − z_min − $2 \cdot mz$) / Δz)
slices $\leftarrow$ empty list
for $k = 0 \ldots K-1$:
$I\_k \leftarrow [z\_min + mz + k \cdot \Delta z, z\_min + mz + (k+1) \cdot \Delta z)$
$S \leftarrow \{ (x,y,z) \in P\_clean \mid z \in I\_k \}$
if $S \neq \emptyset$:
$XY \leftarrow$ projectXY(S)
append to slices: { z = midpoint(I_k), pts = XY, $n = |S|$ }

7) (Optional) Quick visualization
print "> Points after cleaning : |P_clean|"
print "> Number of slices : |slices| ($dz = \Delta z$)"

8) (Optional) Save - save ("preprocessing_output.*",
P_clean, slices,
meta = {
params = { k, Δvoxel, Δz, mz, outlier },
center = c,
rotation= R,

zmin = z_min,
zmax = z_max,
*n*Points = |*P*_clean|
}) END PROCEDURE.

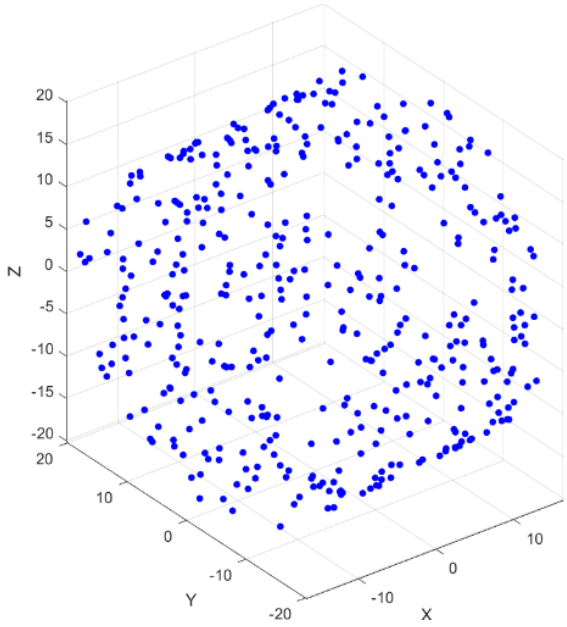

Fig. 5. Pre-processed point cloud

4.3. MULTI-SECTION GEOMETRIC FITTING FOR ADVANCED LOCAL CIRCULARITY EVALUATION

Following the pre-processing steps–which include vertex deduplication, *k*-nearest neighbor filtering with $k = 12$, isotropic voxelization at a resolution of 0.10 mm, reorientation via Principal Component Analysis (PCA) using the principal axis aligned with the *Z*-direction, and axial cropping with a margin of Δz=0.50 mm, the cleaned and aligned point cloud P_{Clean} is segmented into axial slices of constant thickness (0.50 mm). For each level $z = z_k$, lthe set of measured points $s_k = \{(x_i; y_i)\}_{i=1}^{n_k}$ obtained from the scan (excluding CAD data), is projected onto the *XY* plane.

5. SECTIONAL MULTI-SLICE ANALYSIS FOR REFERENCE CIRCLE C_K ESTIMATION AND CIRCULARITY DEVIATION QUANTIFICATION

5.1. ESTIMATION OF THE REFERENCE CIRCLE

The points $(x_i; y_i) \in s_k$ are fitted to the implicit equation of the circle, estimated using linear least squares:

$$(x_i - C_x)^2 + \left(y_i - C_y\right)^2 = R^2 \tag{1}$$

Its expansion yields the linear implicit form in (D, E, and F):

$$x_i{}^2 + y_i{}^2 + D_k x_i + E_k y_i + F_k = 0 \tag{2}$$

Such as $D_k = -2C_{x_i}$; $E_k = -2C_{y_i}$ and $F_k = C_{x_i}^2 + C_{y_i}^2 - R^2$,

The coefficients D, E, and F appear linearly, allowing direct estimation via linear least squares [25]. This step immediately provides the center and radius through straightforward conversion:

$$C_{x_i} = -\frac{D_k}{2} \; ; C_{y_i} = -\frac{E_k}{2} \; ; \; R = \sqrt{\left(C_{x_i}^2 + C_y^2; -F_k\right)} \tag{3}$$

The stacking of the n_k constraints derived from the points of slice S_k leads to an overdetermined linear system:

$$A\theta = -b \tag{4}$$

where: $$A=\begin{bmatrix} x_i & y_i & 1 \\ \vdots & \vdots & \vdots \\ x_{n_i} & y_{n_i} & 1 \end{bmatrix}; \; \theta = \begin{bmatrix} D \\ E \\ F \end{bmatrix} \; ; \; b=\begin{bmatrix} x_i{}^2 + y_i{}^2 \\ \vdots \\ x_{n_k}^2 + y_{n_k}^2 \end{bmatrix} \tag{5}$$

5.2. QUANTIFICATION OF DEVIATIONS AND CIRCULARITY INDICATORS THROUGH SECTIONAL ANALYSIS

For each axial slice $z = z_k$, the local radial deviation of a point $P_i(x_i; y_i)$ is defined as the signed distance separating it from the fitted circle C_k. To obtain a more accurate center and radius, a geometric refinement is applied. This consists in minimizing the sum of the orthogonal distances between all measured points and the reference circle. Starting from an initial estimate $\left(C_x; C_y; R\right)$, the optimization reduces the overall radial deviations and improves the fitting accuracy. The target function to be minimized is expressed as follows:

$$j\ (c_x; c_x; R) = \sum_{i=1}^{n_k} \left(\Delta_{r_i}\right)^2 \tag{6}$$

where $$\Delta_{r_i} = r_i - R \tag{7}$$

and $$r_i = \sqrt{(\mathrm{x}_i - C_x)^2 + \left(y_i - C_y\right)^2} \tag{8}$$

Δ_{r_i}: the local radial deviation of the measured point C_k relative to the section's reference circle,
r_i: radial distance from the measured point $\mathrm{P}_i(x_i; y_i)$ to the slice center $(\mathrm{C_x}; \mathrm{C_y})$,
R: Unique radius of the reference circle to be estimated for the slice.

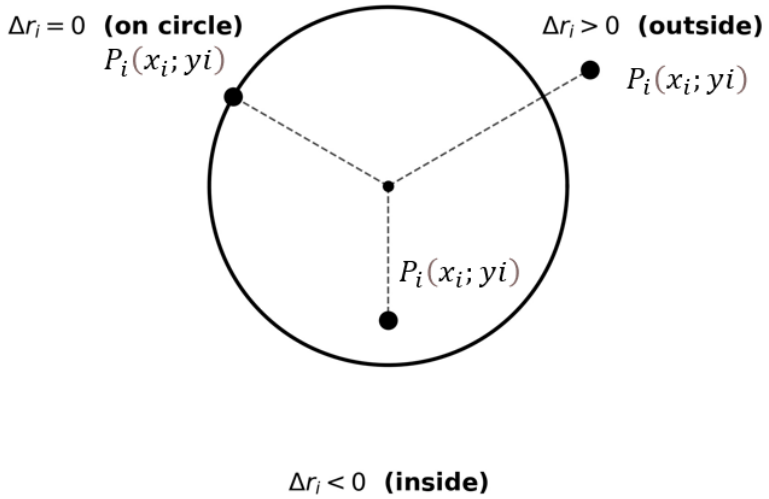

Fig. 6. Illustration of the three cases of $\Delta_{\mathrm{r_i}}$

5.3. INTERPRETATION

The interpretation of Δ_{r_i} characterizes the relative position of a measured point with respect to the fitted circle: a positive value $\Delta_{r_i} > 0$ indicates that the point lies outside the circle, a null value $\Delta_{r_i} = 0$ means that the point lies exactly on the circle, and a negative value $\Delta_{r_i} < 0$ denotes that the point is located inside the circle.

While fitting a circle to the measured points offers an average geometric reference, it doesn't capture the small-scale irregularities within the section. To address this, the Peak-to-Valley (PV) indicator is used. It is defined as the difference between the maximum and minimum values of the radial deviations Δ_{r_i} :

$$PV = \Delta_{r_{i_{max}}} - \Delta_{r_{i_{min}}} \tag{9}$$

This indicator highlights the maximum amplitude of radial dispersion of the measured points relative to the reference circle. It provides a quantitative measure of local circularity, useful for assessing the degree of deformation of a given section compared to an ideal geometry represented by the fitted circle (Fig. 7).

5.2. INTERPRETATION AND DISCUSSION

The analysed section, previously realigned using Principal Component Analysis (PCA), was compared to a reference circle with a constant radius of 20 mm. The observed radial deviations range from −0.542 mm to +0.574 mm, resulting in a peak-to-valley (PV) variation of 1.116 mm. Such an amplitude, exceeding 1 mm, indicates significant geometric distortion and a marked degradation of circularity in this region. The radial profile alternates between radius surplus and deficit, evidencing a lobed geometry and a clear loss of circularity. Using a fixed-radius reference circle isolates intrinsic form errors from dimensional effects, ensuring a rigorous evaluation of local circularity. The resulting high PV deviation thus constitutes a key quantitative indicator of sectional geometric non-conformity, confirming that the deviation exceeds the specified tolerance.

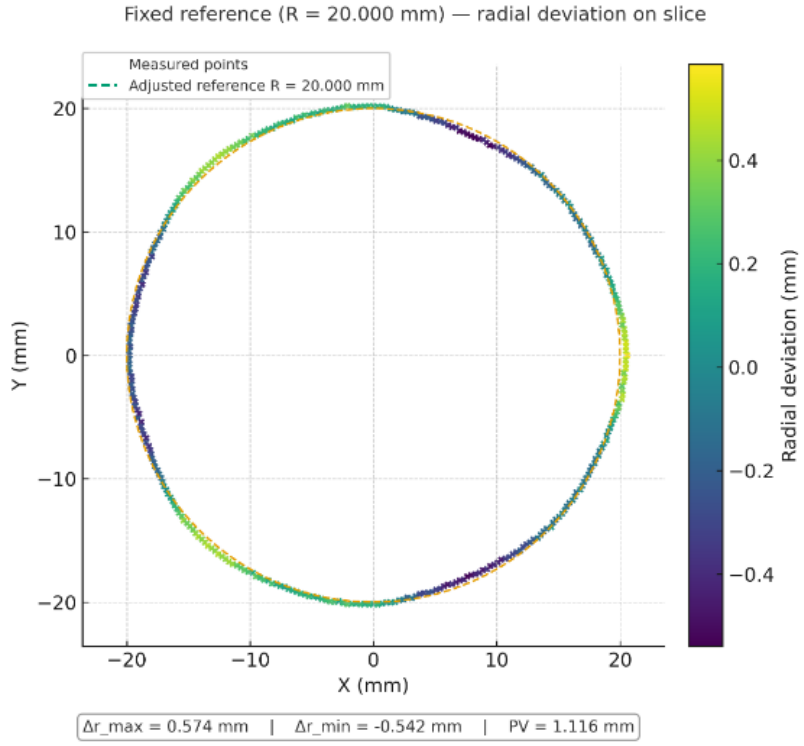

Fig. 7. Circular Fitting with Radial Deviation Assessment in Cross-Section

For comparison, the literature reports that, for FDM parts with nominal dimensions ranging from a few millimetres to a few tens of millimetres, the typical magnitudes of roundness/circularity errors are markedly lower (for instance, “achievable” values around 0.089–0.157 mm depending on the nominal size) [11]. Although the exact criteria (roundness definition, sampling strategy, filtering, and metrological reference) may vary from one study to another, The order-of-magnitude difference observed here supports the conclusion that the investigated region exhibits significant form distortion, which can be attributed to a combination of process-related effects (machine kinematics, local over-/under-extrusion, and

thermo-mechanical shrinkage) and/or factors introduced along the digital-to-metrology workflow.

Finally, it should be emphasized that the use of a 3D scanner and an STL mesh (particularly when the reference STL itself is derived from scanning) may introduce additional error contributions, including discretization (tessellation), optical noise, meshing/smoothing effects, and alignment uncertainties. Recent studies show, on the one hand, that the way the STL is acquired or generated directly influences surface irregularities and the resulting cylindricity deviation values [26], and, on the other hand, that optical scanners remain less suitable for fine form-error assessment than tactile measurements performed on CMMs [27]. In this context, the interpretation of the measured deviations should explicitly account for the combined digital-and-acquisition component, and metrological assurance (verification/ qualification of the optical system) should ideally rely on recognized acceptance and reverification frameworks for optical 3D systems, as well as on the relevant normative requirements applicable to coordinate measuring systems equipped with optical sensors [28].

In our case, the assessment is based on an STL model obtained from a 3D scanner. Consequently, the scan-to-STL workflow, including optical noise, view registration, surface reconstruction, and STL meshing operations such as tessellation, smoothing, and decimation, may alter the radial deviations and therefore directly affect the measured peak-to-valley (PV) value. Moreover, because the PV indicator is defined by extreme values, it is highly sensitive to atypical points (outliers) and may overestimate non-circularity if data pre-processing is not rigorously controlled. To enhance the robustness of the analysis, PV should be complemented with less outlier-sensitive metrics, for example, RMS-based measures, harmonic analysis, or minimum-zone evaluation, particularly in the context of optical measurements [2]. Finally, the reliability of the results depends on the level of verification and qualification of the digitization system, as well as on the proper management of the associated measurement uncertainty, in accordance with the applicable normative frameworks.

6. CONCLUSIONS

The proposed method cleans and organizes the point cloud, duplicate removal, outlier filtering using k-nearest neighbors (k-NN, k = 12), homogenization via voxelization (grid size 0.10 mm), re-centering and alignment through Principal Component Analysis (PCA) with the principal axis aligned along Z, followed by slicing into regular sections (margin 0.50 mm, step 0.50 mm). On each slice, a circle is fitted, the geometric adjustment is refined, and radial deviations of the points from the fitted circle are computed. The peak-to-valley (PV) indicator quantifies the amplitude of these deviations; in our example, PV = 1.116 mm (ranging from −0.542 to +0.574 mm), revealing significant deformation and degraded circularity. As future perspectives. As future work, several methodological improvements are considered. First, a global axis will be estimated from the slice centers using orthogonal regression. Next, an adaptive cylinder will be reconstructed to capture geometric variations along this axis. Cylindricity will then be assessed according to the minimum zone criterion, in compliance with ISO 1101.

ACKNOWLEDGMENTS

Special acknowledgment is extended to the members of the Laboratory of Technology and Industrial Services at the Higher School of Technology of Fez, as well as to those of the Innovation Hub affiliated with Sidi Mohamed Ben Abdellah University in Fez-Morocco, for their valuable contributions and continuous support throughout this research. Their expertise, the relevance of their guidance, and their commitment have been key drivers in the execution and successful completion of this work.

REFERENCES

[1] NGUYEN C.V., DANG L.C., LE A.H., BUI D.T., 2023, *A Study on the Influence of Printing Orientation in Metal Printing Using Material Extrusion Technology on the Mechanical Properties of 17-4 Stainless Steel Products*, Journal of Machine Engineering, https://doi.org/10.36897/jme/170509.

[2] SWIDERSKI J., MAKIELA W., DOBROWOLSKI T., STĘPIEN K., ZUPERL U., 2022, *The Study of the Roundness and Cylindricity Deviations of Parts Produced with the Use of the Additive Manufacturing*, Int. J. Adv. Manuf. Technol., 121/11-12, 7427–7437, https://doi.org/10.1007/s00170-022-09838-1.

[3] SAHU A., NAGARGOJE A., TANDON P., 2022, *Feature Segmentation of Multifeatured Freeform Geometries for Incremental Sheet Forming*, Digital Manufacturing Technology, 65–77, https://doi.org/10.37256/dmt.2220221859.

[4] JAFARZADEH S., COMMINAL R., SERDECZNY M.P., BAYAT M., BAHL C.R.H., SPANGENBERG J., 2023, *Geometric Characterization of Orthogonally Printed Layers in Material Extrusion Additive Manufacturing: Numerical Modeling and Experiments*, Progres dans la fabrication additive, 8, 1619–1630.

[5] NGO T.D., KASHANI A., IMBALZANO G., NGUYEN K.T.Q., HUI D., 2018, *Additive Manufacturing (3D Printing): A Review of Materials, Methods, Applications and Challenges*, Composites Part B: Engineering, 143, 172–196, https://doi.org/10.1016/j.compositesb.2018.02.012.

[6] PETERKA J., 2024, *Research of Layer Thickness and Selected Thermoplastic Materials and Their Influence on the Surface Roughness in the Process of Fused Deposition Modeling Technology*, Journal of Electrical Systems, 20, 758–765, https://doi.org/10.52783/jes.2099.

[7] PETRUSE R.E., SIMION C., BONDREA I., 2024, *Geometrical and Dimensional Deviations of Fused Deposition Modelling (FDM) Additive-Manufactured Parts*, Metrology, 4/3, 411–429, https://doi.org/10.3390/metrology4030025.

[8] CHAHBOUNI M., 2016, *Contribution to the Design of Mechanisms: Tolerance Analysis with the Influence of Form Defects*, PhD Thesis, Morocco.

[9] SASALA M., HRIVNIAK L., SVETLIK J., DEMEC P., 2020, *Compensation for Deviations on Cylindrical Shapes Manufactured by 3D Printers*, MM SJ, 2, 3896–3899, https://doi.org/10.17973/MMSJ.2020_06_2019149.

[10] FAHAD M., KHALID M., NAUMAN M., KHAN M.A., 2017, *Effect of Deposition Speed on the Flatness and Cylindricity of Parts Produced by Three-Dimensional Printing Process*, J. Phys.: Conf. Ser., 885, 012012, https://doi.org/10.1088/1742-6596/885/1/012012.

[11] SOOD A.K., OHDAR R.K., MAHAPATRA S.S., 2010, *Parametric Appraisal of Mechanical Property of Fused Deposition Modelling Processed Parts*, Materials & Design, 31/1, 287–295, https://doi.org/10.1016/j.matdes.2009.06.016.

[12] EL-QEMARY A., KABBOURI I., BOUTAHARI S., CHAHBOUNI M., 2025, *Anticipation and Correction of Additive Manufacturing Geometric Defects at the Design Stage* , Journal of Machine Engineering, 25/2, 74–88, https://doi.org/10.36897/jme/204662.

[13] NGUYEN T.T., TRAN T.V., DAO S.H., 2024, *A Study on the Ability to Fabricate Mold Using 3D Printing Technology and Evaluate the Surface Roughness of Products in Investment Casting*, Journal of Machine Engineering, 24/3, 106–118, https://doi.org/10.36897/jme/189942.

[14] ZHU Z., ANWER N., MATHIEU L., 2017, *Deviation Modeling and Shape Transformation in Design for Additive Manufacturing*, Procedia CIRP, 60, 211–216, https://doi.org/10.1016/j.procir.2017.01.023.

[15] TAO Q, FU B., ZHON F. 2025, *A Review of Challenges and Future Perspectives for High-Speed Material Extrusion Technology*, MDPI.

[16] KABBOURI I., et al, 2025, *Modelling Geometric Deviations in Additive Manufacturing of a Cylindrical Surface*, Journal of Machine Engineering, https://doi.org/10.36897/jme/211736.

[17] SHAKERI Z., et al., 2021, *Mathematical Modeling and Optimization of Fused Filament Fabrication (FFF) Process Parameters for Shape Deviation Control of Polyamide 6 Using Taguchi Method*, Polymers, 13/21, https://doi.org/doi/10.3390/polym13213697.

[18] RUSU R.B., COUSINS S., 2011, *3D is Here: Point Cloud Library (PCL)*, 2011 IEEE International Conference on Robotics and Automation, Shanghai, China: IEEE, 1–4, https://doi.org/10.1109/ICRA.2011.5980567.

[19] RUCHAY A.N., et al., 2019, *Accuracy Analysis of 3D Object Reconstruction Using Point Cloud Filtering Algorithms*, in Proceedings of the V International conference Information Technology and Nanotechnology, IP Zaitsev V.D., 169–174, https://doi.org/doi/10.18287/1613-0073-2019-2391-169-174.

[20] HUANG X., et al., 2022, *Robust Real-World Point Cloud Registration by Inlier Detection*, Computer Vision and Image Understanding, 224, 103556, https://doi.org/doi/10.1016/j.cviu.2022.103556.

[21] ZU H., et al., 2025, *Research on Self-Adaptive Grid Point Cloud Down-Sampling Method Based on Plane Fitting and Mahalanobis Distance Gaussian Weighting*, Neurocomputing, 634, 129746, https://doi.org/doi/10.1016/j.neucom.2025.129746.

[22] BERGAMASCO F., PISTELLATO M., ALBARELLI A., TORSELLO A., 2020, *Cylinders Extraction in Non-Oriented Point Clouds as a Clustering Problem*, Pattern Recognition, 107, 107443, https://doi.org/doi/10.1016/j.patcog.2020.107443.

[23] LIU F. et al., 2023, *An Iterative Minimum Zone Algorithm for Assessing Cylindricity Deviation*, Measurement, 213, 112738, https://doi.org/doi/10.1016/j.measurement.2023.112738.

[24] CHENG R., JIAN H., LI Y., HUANG Q., ZHANG L., LI H., 2025, *A Novel Minimum Zone Method for Cylindricity Error Evaluation Based on Rotation Projection Method and Adaptive Particle Swarm Optimisation*, Precision Engineering, 94, 149–158, https://doi.org/doi/10.1016/j.precisioneng.2025.02.025.

[25] LI Q., GE W., SHI H., ZHAO W., ZHANG S., 2024, *Research on Coaxiality Measurement Method for Automobile Brake Piston Components Based on Machine Vision*, Applied Sciences, 14/6, 2371, https://doi.org/doi/10.3390/app14062371.

[26] ZMARZLY P., SZCZYGIEL P., BUJARSKA A., 2025, *Impact of STL File Format on the Cylindricity Deviation of Models Manufactured Using FDM Technology*, Metrology and Measurement Systems, 1–15, https://doi.org/doi/10.24425/mms.2025.154673.

[27] BUJARSKA A., ZMARZLY P., SZCZYGIEL P., 2025, *Application of Optical Measurements to Assess form Deviations of Cylindrical Parts Made Using FDM Additive Technology*, Sensors, 25/18, https://doi.org/doi/10.3390/s25185855.

[28] ISO 10360-8:2013, ISO, 2025, *Geometrical Product Specifications (GPS) – Acceptance and Reverification Tests for Coordinate Measuring Systems (CMS) – Part 8: Coordinate Measuring Machines (CMMs) with Optical Distance Sensors*.